Progress In Electromagnetics Research Letters, Vol. 89, 99–104, 2020

A Broadband Microstrip-to-Waveguide End-Wall Probe Transition and Its Application in Waveguide Termination

Cong Tang[1], Xiaofeng Pan[1], Fei Cheng[2, *], and Xian Qi Lin[3]

Abstract—A broadband microstrip-to-waveguide end-wall probe transition using a semicircular loop is proposed in this letter. The simulated 20-dB fractional bandwidth for this transition is 48.3% which could cover the whole *Ka*-band. Then, a compact broadband waveguide termination is developed by combination of this microstrip-to-waveguide transition and a 50 Ω microstrip termination. To reduce parasitic effects, the microstrip termination is grounded by a microstrip radial stub. The fabricated waveguide termination shows a compact size and has a return loss better than 16.6 dB from 26 to 40.8 GHz.

1. INTRODUCTION

Waveguide is the most popular transmission line in millimeter-wave band for its low insertion loss [1]. However, it cannot be directly connected to microwave chips. To solve this problem, microstrip-to-waveguide transition which has the ability to integrate the waveguide with the planner passive and active circuits is proposed [2]. A good microstrip-to-waveguide must have broad bandwidth, low insertion loss, and compact size [3–12]. Generally, the microstrip-to-waveguide transition can be divided into two types. One is orthogonal transition [3–5], and the other is in-line transition [6–12]. Since an additional quarter-wavelength waveguide backshort is needed in the orthogonal transition, the orthogonal transition has a larger size than the in-line transition. Thus, the in-line transition is more preferred in most designs.

Waveguide termination is a one-port device which is used to absorb input microwave signals with no reflection [1]. High performance waveguide terminations which show compact size and broad bandwidth are widely used in applications such as waveguide directional couplers, hybrids, and circulators. Moreover, the waveguide terminations also play an important role in the short-open-load-thru (SOLT) calibration of the scattering parameters measurement.

The conventional waveguide terminations are usually manufactured using lossy materials with a gradual shape such as a pyramid [13], multiple steps [14], and tapered-wedges [15, 16]. The bandwidth of the termination is related to the length of lossy materials. To achieve a wider bandwidth, the longitudinal dimension of the termination remains long. In [17], short waveguide termination was achieved by a metamaterial absorber. However, due to the resonant structure of the metamaterial, the fabricated waveguide termination only exhibits narrow bandwidth.

In this work, a *Ka*-band semicircular loop coupled microstrip-to-waveguide end-wall transition is firstly designed. It belongs to the inline transition which exhibits a compact size. The fabricated back-to-back microstrip to waveguide transition shows a broad bandwidth from 25 to 43 GHz for the return loss better than 15 dB. Then, a microstrip termination is achieved by a thin film chip resistor and a

Received 6 November 2019, Accepted 29 December 2019, Scheduled 22 January 2020
* Corresponding author: Fei Cheng (chengfei@scu.edu.cn).
[1] Nanjing Electronic Devices Institute, Nanjing, Jiangsu 210016, China. [2] Key Laboratory of Wireless Power Transmission Ministry of Education, College of Electronics and Information Engineering, Sichuan University, Chengdu, Sichuan 610065, China. [3] EHF Key Lab of Fundamental Science, School of Electronic Engineering, University of Electronic Science and Technology of China, Chengdu 611731, China.

radial stub which works as the RF ground. By combining the microstrip to waveguide transition and the microstrip termination, a broadband waveguide termination is achieved. Different from the previous works, the longitudinal dimension of the waveguide termination in this work is mainly dependent on the length of the microstrip to waveguide transition. The fabricated termination shows a compact size and has a wide fractional bandwidth of 41.3% for the return loss better than 16.6 dB.

2. MICROSTRIP-TO-WAVEGUIDE TRANSITION USING SEMICIRCULAR LOOP

The proposed *Ka*-band microstrip-to-waveguide transition is shown in Fig. 1. As shown, the transition consists of three parts, which are a rectangular waveguide, a semicircular loop, and a microstrip matching circuit. The rectangular waveguide is a standard WR-28 waveguide with the dimension of 7.112 mm × 3.556 mm, which will ensure single TE_{10} mode propagation in the *Ka*-band. The semicircular loop and microstrip matching circuit are fabricated on a Rogers 5880 substrate (relative dielectric constant = 2.2, loss tangent = 0.0009, copper thickness = 0.017 mm, substrate thickness = 0.127 mm). The semicircular loop, which acts as an impedance transformer, is placed at the *E*-plane of the rectangular waveguide. So the semicircular loop is perpendicular to the direction of the magnetic field lines, and the magnetic field lines pass through the semicircular loop. The microwave energy is coupled to the semicircular loop magnetically. The semicircular loop works as a loop antenna. The initial design parameters for the loop are set to be one wavelength at the center frequency (33 GHz) of the working band (*Ka* band) which is about 9.1 mm. Then, those parameters are optimized in HFSS. The microstrip matching circuit, which has two sections of different characteristic impedance microstrip

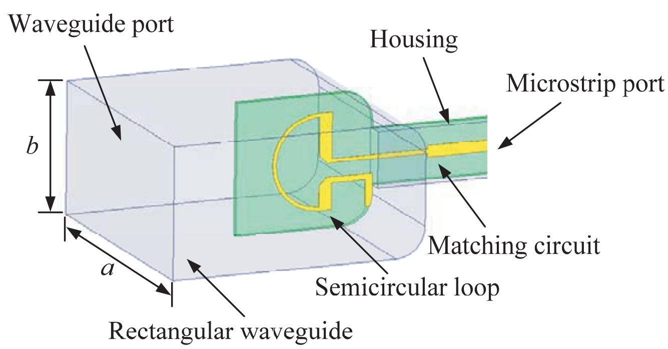

Figure 1. Structure of the proposed microstrip-to-waveguide transition.

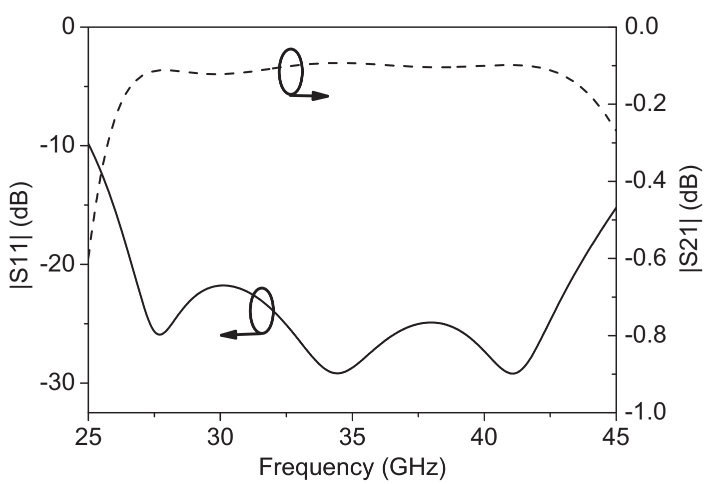

Figure 2. Simulated *S*-parameters of the microstrip-to-waveguide transition.

lines, is packaged with a metal housing. The cross-sectional dimension of the housing is chosen as 1.5 mm × 0.5 mm, hence there is no waveguide mode propagating in the housing when the transition operates in the *Ka*-band.

The insertion loss and return loss of the microstrip-to-waveguide transition are simulated by the commercial software ANSYS HFSS 15 which is finite element method (FEM) field solver. Fig. 2 illustrates the simulated results. As shown, the return loss is better than 20 dB rangeing from 26.65 to 43.62 GHz with a fractional bandwidth of 48.3%. The corresponding insertion loss in this frequency range is lower than 0.13 dB.

To verify the design, a back to back microstrip-to-waveguide transition using the semicircular loop is fabricated and measured. The layout of the planar circuit with dimensions is shown in Fig. 3. A photograph of the fabricated transition is shown in Fig. 4(a). Fig. 4(b) compares the simulated and measured results of the transition which agree with each other very well. The measured insertion loss of the transition is lower than 0.9 dB in the whole *Ka*-band while the measured return loss is lower than 15 dB in the whole *Ka*-band. Table 1 compares our work with previous ones. It can be seen that the transition in this work has a broader bandwidth than other designs. It shows a little larger insertion loss than some designs. One reason is that the microstrip line has a larger insertion loss at higher frequencies.

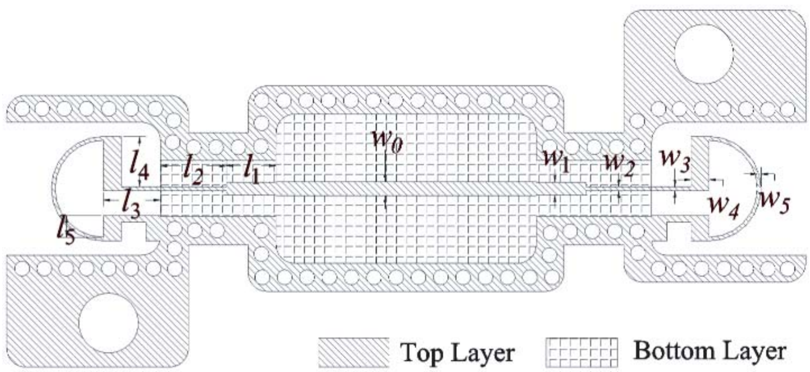

Figure 3. Layout of the planar circuit for the *Ka*-band back to back microstrip-to-waveguide transition with dimensions. ($l_1 = 1.34$, $l_2 = 1.77$, $l_3 = 1.54$, $l_4 = 1.35$, $l_5 = 0.58$, $w_0 = 0.37$, $w_1 = 0.34$, $w_2 = 0.11$, $w_3 = 0.1$, $w_4 = 0.48$, $w_5 = 0.1$, unit: mm).

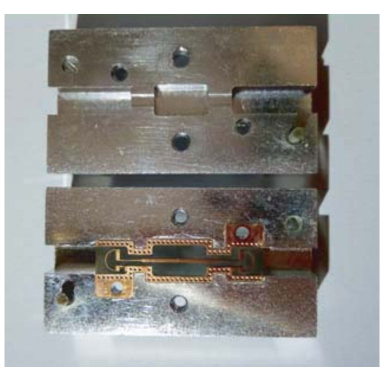

(a)

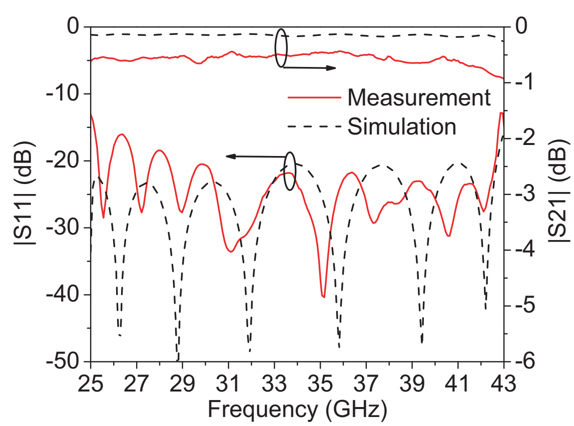

(b)

Figure 4. (a) Photograph of the fabricated back to back microstrip-to-waveguide transition. (b) Simulated and measured *S*-parameters of the back to back microstrip-to-waveguide.

Table 1. Comparison between this work and other published microstrip-to-waveguide transitions.

Refs.	Frequency range (GHz)	Relative bandwidth (%)	Return loss (dB)	Insertion loss (dB)
[8]	8–13	47.4	> 15	< 0.22
[10]	8–12.5	26	> 15	< 0.7
[11]	8–10	11.11	> 10	< 2.2
[12]	9.4–12.7	33	> 15	NG
This work	25–43	51.73	> 15	< 0.9

3. MILLIMETER-WAVE MICROSTRIP TERMINATION

The microstrip termination as shown in Fig. 5 consists of three parts including a $50\,\Omega$ microstrip line, a $50\,\Omega$ chip resistor, and a radial stub. The same Rogers 5880 substrate in the microstrip-to-waveguide transition design is used here. The $50\,\Omega$ thin film resistor is from Vishay with a 0402 package [18]. Due to its small size, the resistor shows low parasitic effects up to 40 GHz. The RF ground is a 90° radial stub instead of a metallic via. On one hand, the metallic via has unacceptable large parasitic effects at *Ka*-band, leading to rather narrow bandwidth. On the other hand, the radial stub can be equal to a small capacitor which is short for broadband RF signals. The cross-sectional dimension of the housing for the microstrip termination is $4\,\text{mm} \times 1.6\,\text{mm}$. ANSYS HFSS 15 is used in the simulation. The metal house is used in the simulation. The simulated return loss of the microstrip termination is better than 20 dB from 25.39 to 42.61 GHz as shown in Fig. 5.

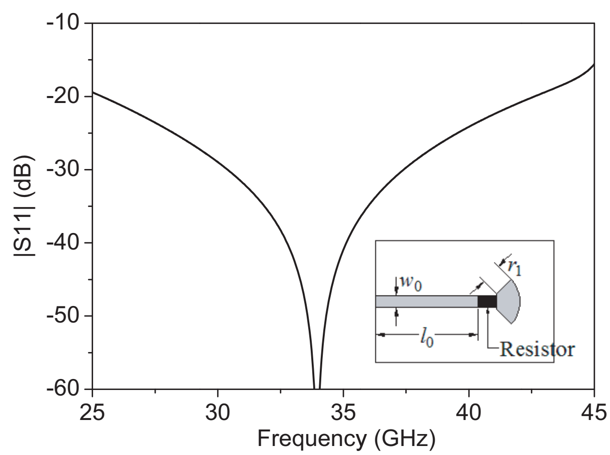

Figure 5. Structure and simulated reflection coefficient of the microstrip termination. ($w_0 = 0.37$, $l_0 = 3.35$, $r_1 = 0.67$, unit: mm).

4. WAVEGUIDE TERMINATION FABRICATION AND MEASUREMENT

Combining the microstrip-to-waveguide transition in Section 2 and the microstrip termination in Section 3, we can get the waveguide termination. Fig. 6 shows the layout of the planar circuit for the waveguide termination. The simulated and measured results as well as the photograph of the waveguide termination are shown in Fig. 7. As shown, the measured return loss is better than 16.6 dB in the frequency range of 26.3 to 40 GHz which is 41.3% fractional bandwidth. Compared with the simulation, the measured return loss degrades about 10 dB which is estimated to be caused by the fabrication and assemble errors.

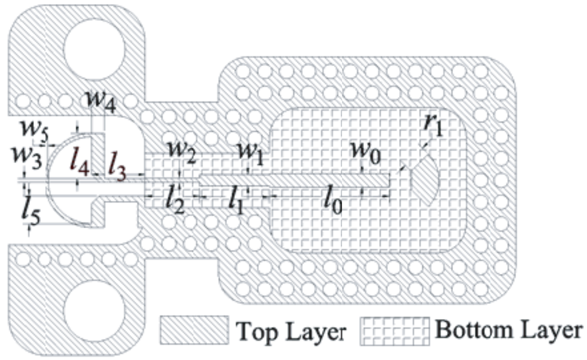

Figure 6. Layout of the planar circuit for the proposed termination with dimensions. ($l_0 = 3.35$, $l_1 = 1.93$, $l_2 = 1.53$, $l_3 = 1.48$, $l_4 = 1.25$, $l_5 = 0.77$, $w_0 = 0.37$, $w_1 = 0.31$, $w_2 = 0.12$, $w_3 = 0.1$, $w_4 = 0.35$, $w_5 = 0.1$, $r_1 = 0.67$, unit: mm).

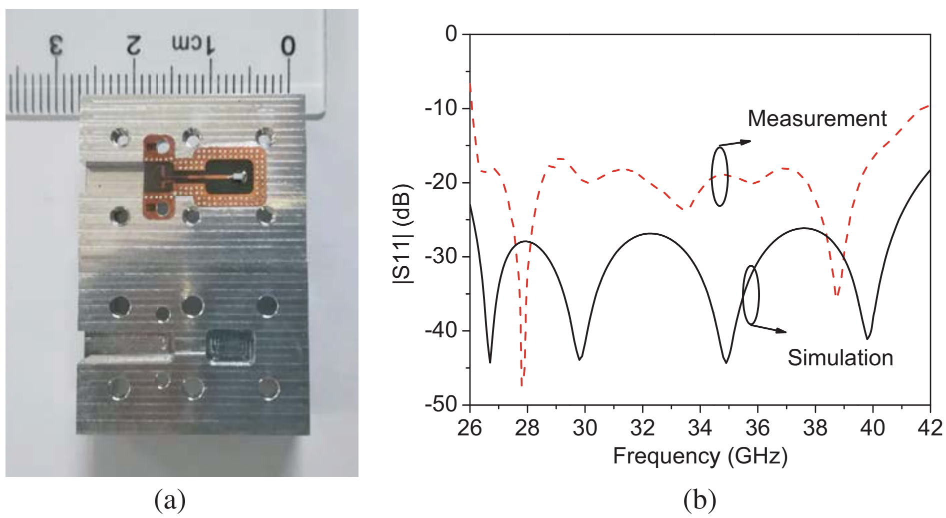

Figure 7. (a) Photograph of the fabricated waveguide termination. (b) Measured and simulated results of the waveguide termination.

5. CONCLUSION

A broadband microstrip to waveguide end-wall probe transition working in the *Ka*-band is presented. Based on this transition, a compact and broadband waveguide termination is realized. A thin film resistor is used as the load of the termination. Except for the application of waveguide termination, the microstrip to waveguide transition can also be used in other millimeter-wave circuit designs. The potential of the proposed waveguide termination is demonstrated for the application in high performance, low profile, and low cost RF-front-ends.

ACKNOWLEDGMENT

This work was supported in part by the National Natural Science Foundation of China (Grant No. 61801317) and in part by Sichuan University Postdoctoral Interdisciplinary Innovation Start-up fund project.

REFERENCES

1. Pozar, D. M., *Microwave Engineering*, Wiley, New York, 2005.
2. Hoover, J. C. and R. E. Tokheim, "Microstrip transmission-line transitions to dielectric-filled waveguide," *IEEE Trans. Microw. Theory Tech.*, Vol. 15, No. 4, 273–274, Apr. 1967.
3. Oh, H. S. and K. W. Yeom, "A full Ku-band reduced-height waveguide-to-microstrip transition with a short transition length," *IEEE Trans. Microw. Theory Tech.*, Vol. 58, No. 9, 2456–2462, Sep. 2010.
4. Häseker, J. S. and M. Schneider, "90 degree microstrip to rectangular dielectric waveguide transition in the W-band," *IEEE Microw. Wireless Compon. Lett.*, Vol. 26, No. 6, 416–418, Jun. 2016.
5. Aliakbarian H., A. Enayati, G. A. E. Vandenbosch, and W. de Raedt, "Novel low-cost end-wall microstrip-to-waveguide splitter transition," *Progress In Electromagnetics Research*, Vol. 101, 75–96, 2010.
6. Kaneda, N., Y. Qian, and T. Itoh, "A broadband microstrip-to-waveguide transition using quasi-Yagi antenna," *IEEE Trans. Microw. Theory Tech.*, Vol. 47, No. 12, 2562–2567, Dec. 1999.
7. Huang, X. and K. L. Wu, "A broadband U-slot coupled microstrip-to-waveguide transition," *IEEE Trans. Microw. Theory Tech.*, Vol. 60, No. 5, 1210–1217, May 2012.
8. Chuang, J. K., R. Y. Fang, and C. L. Wang, "Compact and broadband microstrip-to-waveguide transition using antisymmetric tapered probes," *Electron. Lett.*, Vol. 48, No. 6, 332–333, Mar. 2012.
9. Fang, R. Y. and C. L. Wang, "Miniaturized microstrip-to-waveguide transition using capacitance-compensated broadside-coupled microstrip line," *IEEE Trans. Compon. Packag. Manuf. Technol.*, Vol. 3, No. 9, 1588–1596, Sep. 2013.
10. Jokanovic, B. and D. Markovic, "Wideband microstrip-to-waveguide transition using double-Y balun," *Electron. Lett.*, Vol. 42, No. 18, 1043–1044, Aug. 2006.
11. Zhang, Y. C., J. A. Ruiz-Cruz, K. A. Zaki, and A. J. Piloto, "A waveguide to microstrip inline transition with very simple modular assembly," *IEEE Microw. Wireless Compon. Lett.*, Vol. 20, No. 9, 480–482, Sep. 2010.
12. Risacher, C., V. Vassilev, A. Pavolotsky, and V. Belitsky, "Waveguide-to-microstrip transition with integrated bias-T," *IEEE Microw. Wireless Compon. Lett.*, Vol. 13, No. 7, 262–264, Jul. 2003.
13. Arbaoui, Y., V. Laur, A. Maalouf, et al., "Full 3-D printed microwave termination: A simple and low-cost solution," *IEEE Trans. Microw. Theory Tech.*, Vol. 64, No. 1, 271–278, Jan. 2016.
14. Monge, F. J., J. Esteban, and J. Zapata, "Finite elements and evolution programs for the CAD of broadband rectangular-waveguide H-plane matched loads," *Microw. Opt. Technol. Lett.*, Vol. 31, No. 6, 491–494, 2001.
15. Stander, T., P. W. van derWalt, and P. Meyer, "A comparison of simple low-power wedge-type X-band waveguide absorbing load implemen-tations," *AFRICON 2007*, 1–4, Windhoek, Namibia, Sep. 2007.
16. Komarov, V. V., V. P. Meschanov, and N. F. Popova, "Short waveguide load for millimetre-wave applications," *Electron. Lett.*, Vol. 52, No. 5, 378–379, 2016.
17. Li, J., G. Wen, Y. Huang, P. Wang, and Y. Sun, "Research of metamaterial absorbers and their rectangular waveguide matching terminal applications based on the electric resonators," *Acta. Phys. Sin.*, Vol. 62, No. 8, 087801-1–087801-7, 2013.
18. Vishay Intertechnology, "High frequency (up to 40 GHz) resistor, thin film surface mount chip," http://www.vishay.com/doc?60093, Feb. 17, 2008.